

SUPPORTING INFORMATION

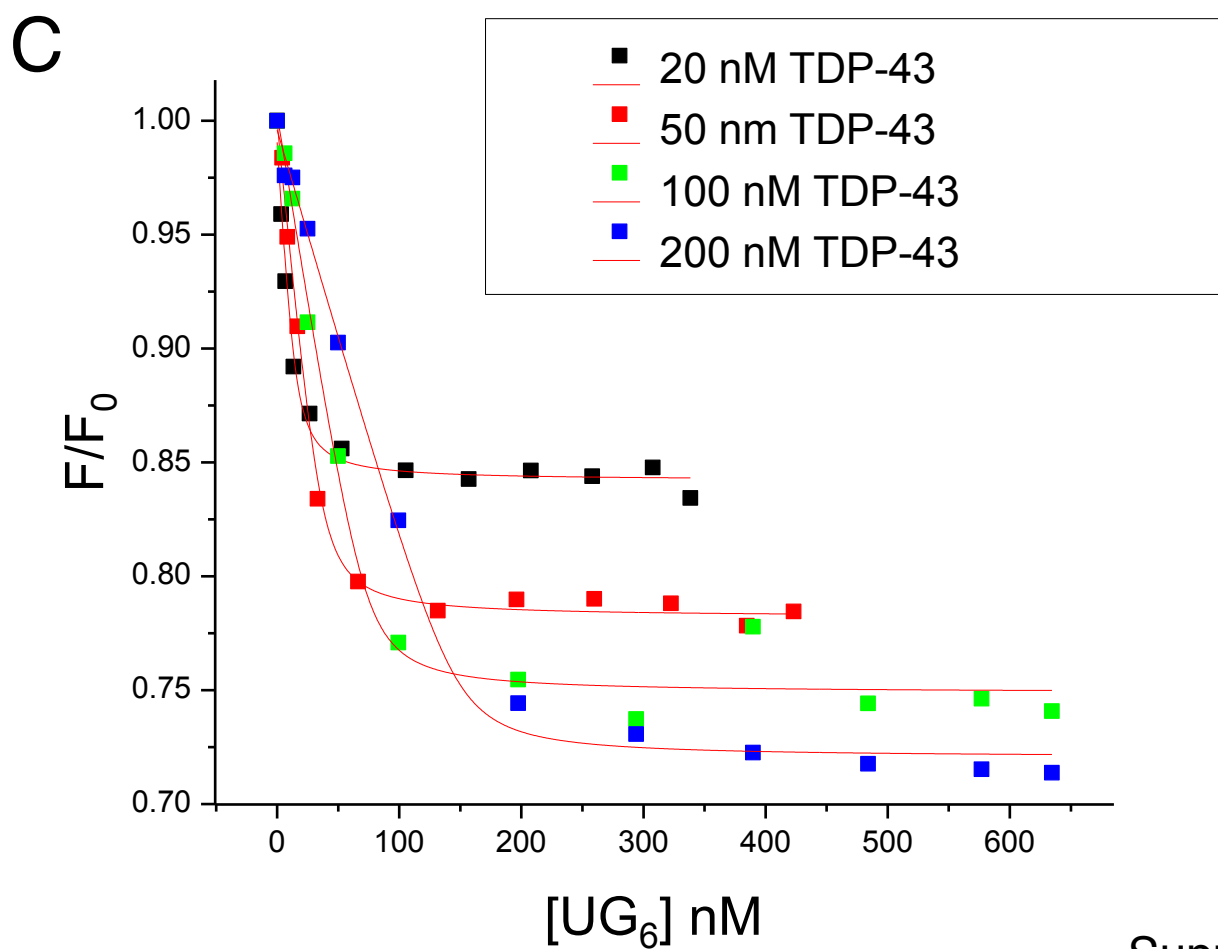
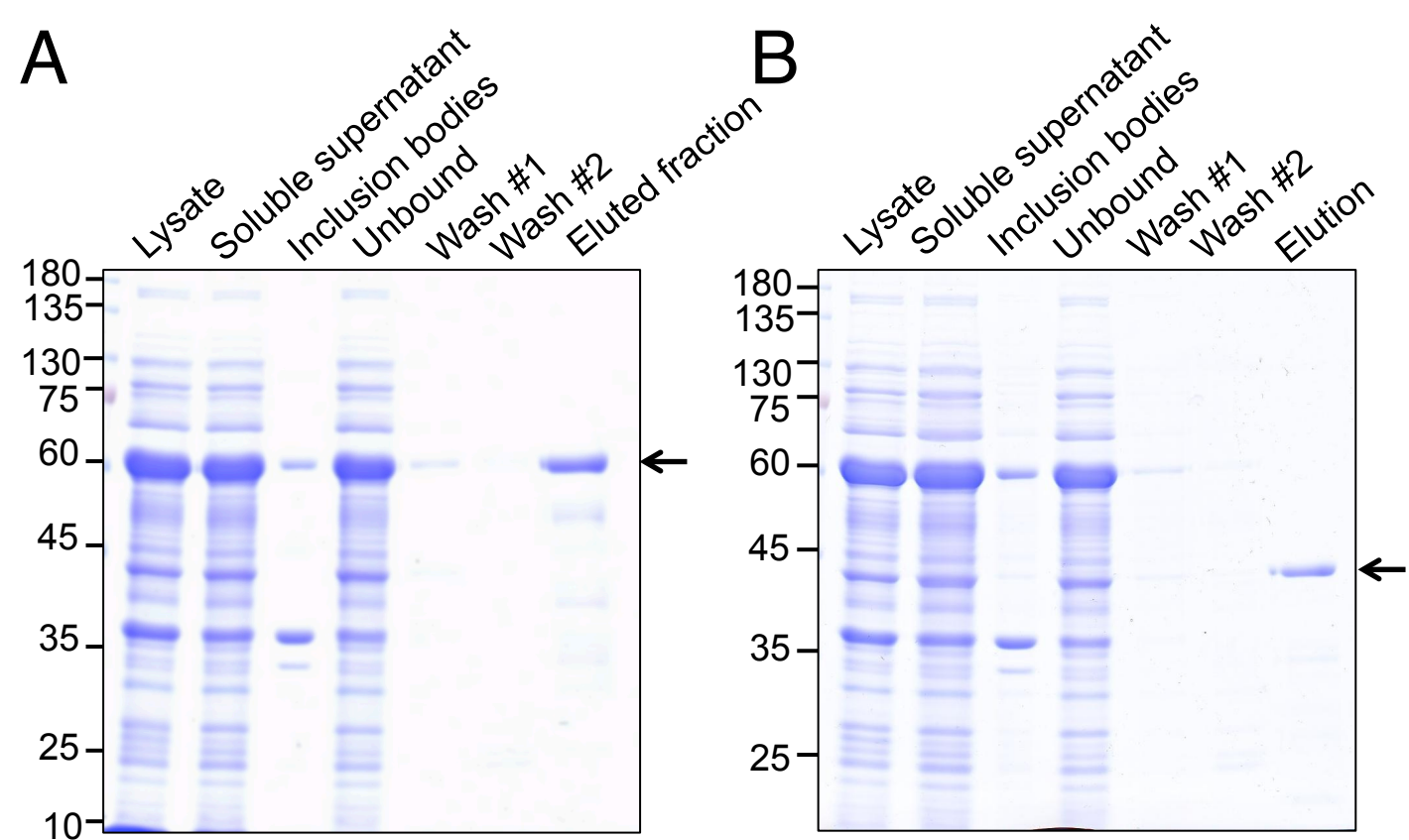
TDP-43 oligomers detected as initial intermediate species during aggregate formation

Rachel L. French, Zachary Grese, Himani Aligireddy, Dhruva D. Dhavale, Ashley N. Reeb, Niraja Kedia, Paul T. Kotzbauer, Jan Bieschke, and Yuna M. Ayala

1. Supporting Table
2. Supporting Figure
3. Supporting Figure Legends

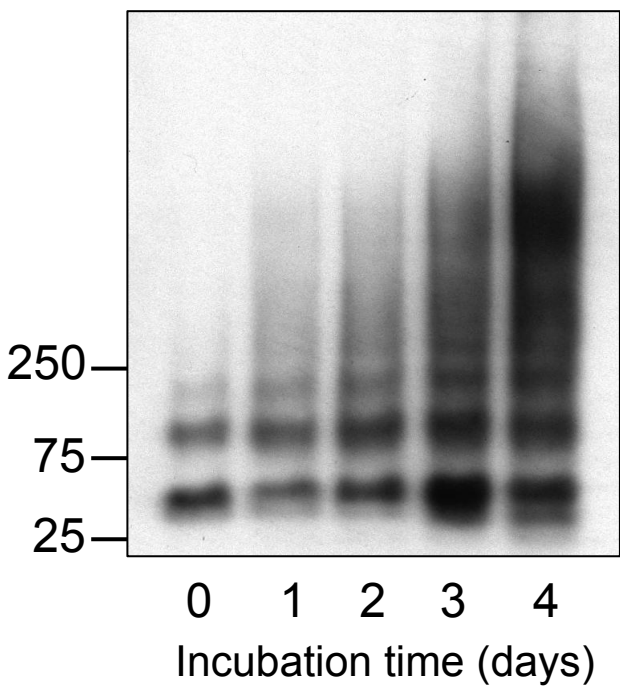
Supporting Table List and sequence of oligonucleotides used for cloning and mutagenesis.

Name	Sequence
Bam_102 FW	5'-CGCGGATCCAAAACATCCGATTTAATAG-3'
Sac_269 RV	5'-GATCGAGCTCCTACTGTCTATTGCTATTGTG-3'
A315T FW	5'-GATGAACTTTGGTACGTTTCAGCATTAAATC-3'
A315T RV	5'-GATTAATGCTGAACGTACCAAAGTTCATC-3'
M337V FW	5'-CAGAGCAGTTGGGGTATGGTGGGCATGTTAGCCAGCCAG-3'
M337V RV	5'-CTGGCTGGCTAACATGCCACCATAACCCCAACTGCTCTG-3'
Hind_HA_mcherry F	5'-GACTGAAGCTTGCAATGTACCCATACGATGTTCCCGACTAC GCCGTGAGCAAGGGCGAGGAGGATAAC-3'
BamH_mCherry R	5'-CATGCGGATCCCTTGTACAGCTCGTCCATG-3'
BamH_TDP FW	5'-CATGCGGATCCTCTGAATATATTCGGGTAACCG-3'
Not_TDP RV	5'-AAGGAAAAAAGCGGCCGCCTACATTCCCCAGCCAGAAGAC-3'
NLS1 FW	5'-AACTATCCAAAAGATAACGCCGCTGCGATGGATGAGACAG ATGCTTC-3'
NLS1 RV	5'-GAAGCATCTGTCTCATCCATCGCAGCGGCGTTATCTTTTGG ATAGTTG-3'
TDP101-mEGFP FW	5'-AAAAGAGCAGTCCAGATGGTGAGCAAGGGC-3'
TDP101-mEGFP RV	5'-GGCCTTGCTCACCATCTGGACTGCTCTTTT-3'
mEGFP-TDP261 FW	5'-GACGAGCTGTACAAGGAACCTAAGCACAAT-3'
mEGFP-TDP261 RV	5'-ATTGTGCTTAGGTTCCCTTGTACAGCTCGTC-3'
Y4R FW	5'-AGATTGGTGGATCCTCTGAACGTATTCGGGTAACCGAAGATG-3'
Y4R RV	5'-CATCTTCGGTTACCCGAATACGTTTCAGAGGATCCACCAATCT-3'
E17R FW	5'-AGAACGATGAGCCCATTCGAATACCATCGGAAGACGATG-3'
E17R RV	5'-CATCGTCTTCCGATGGTATTCGAATGGGCTCATCGTTCT-3'



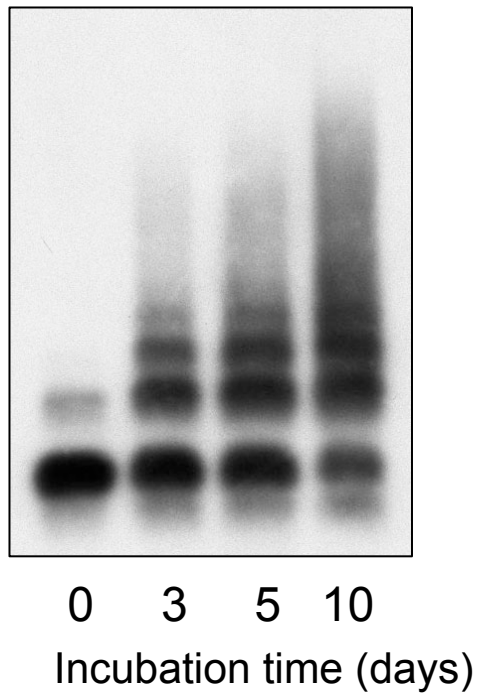
A

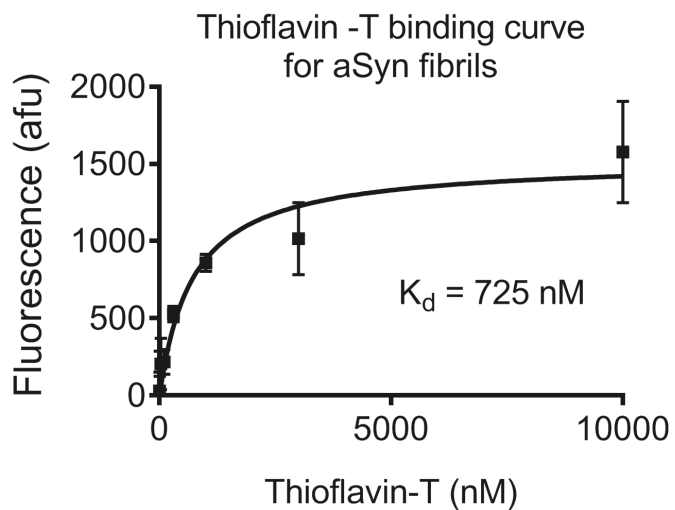
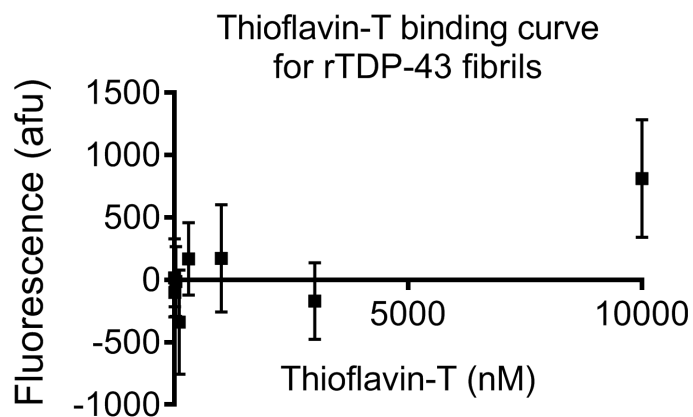
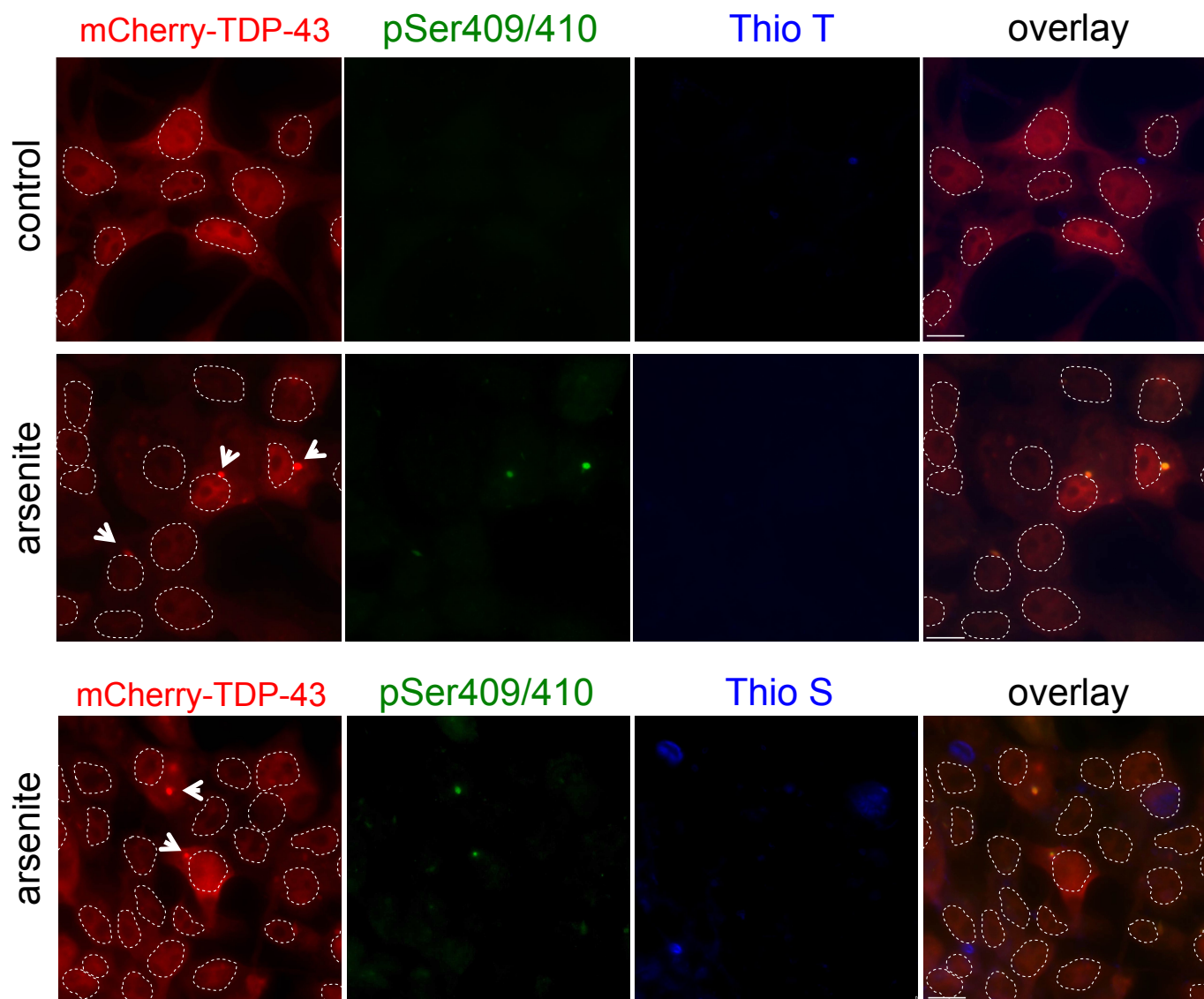
0.7% PEG



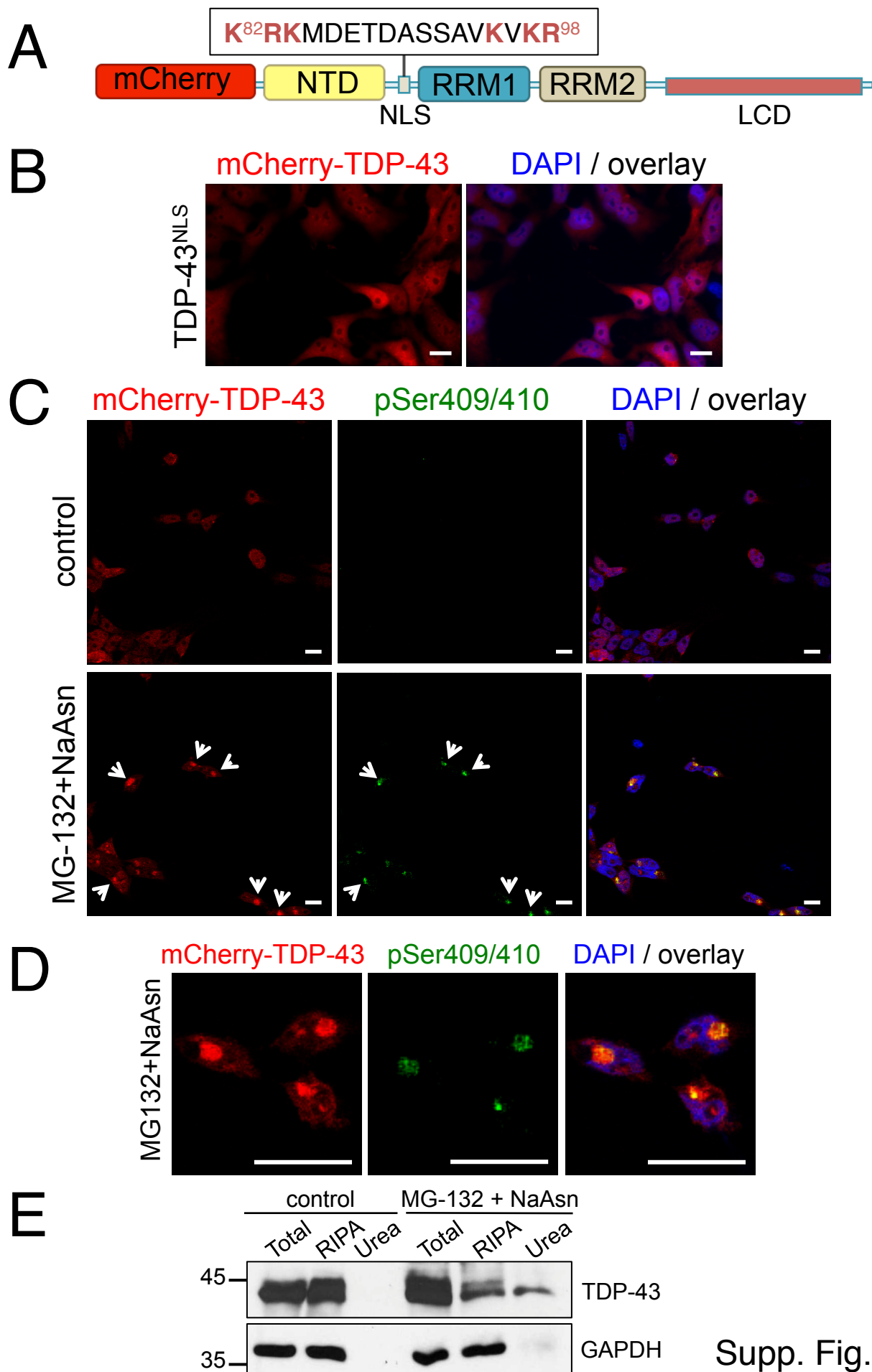
B

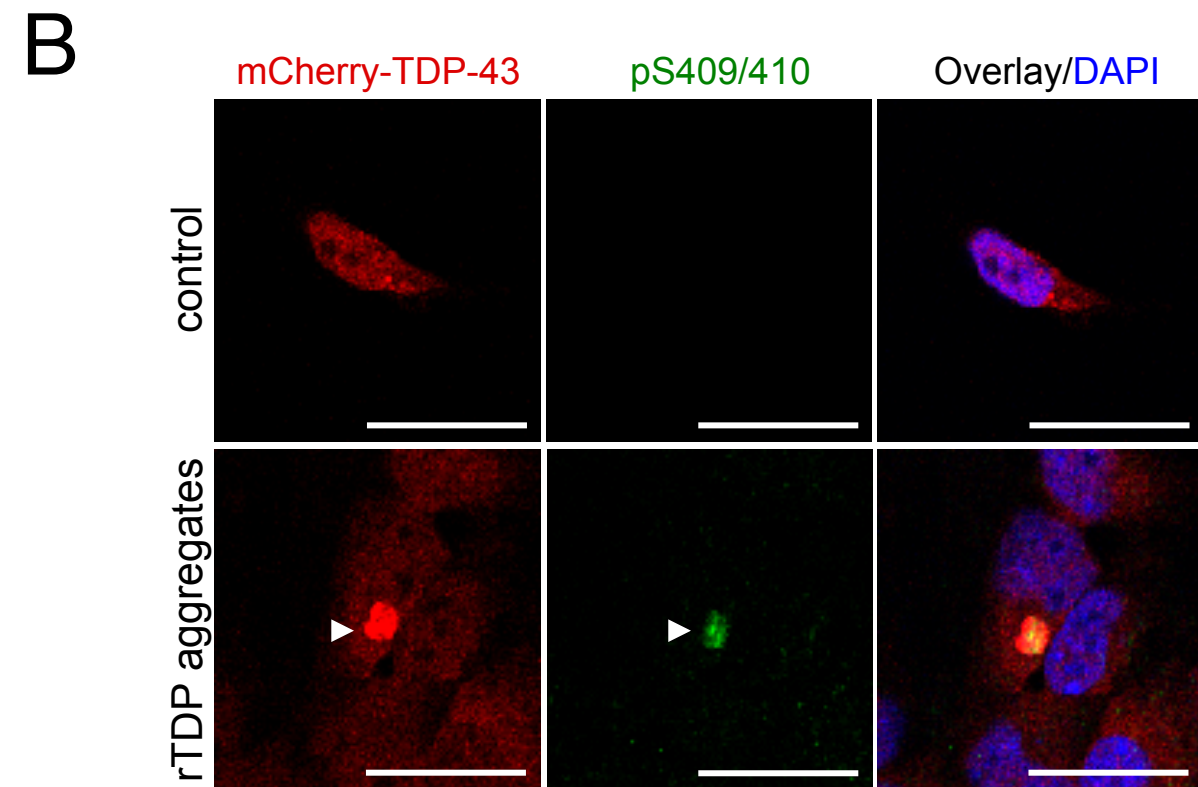
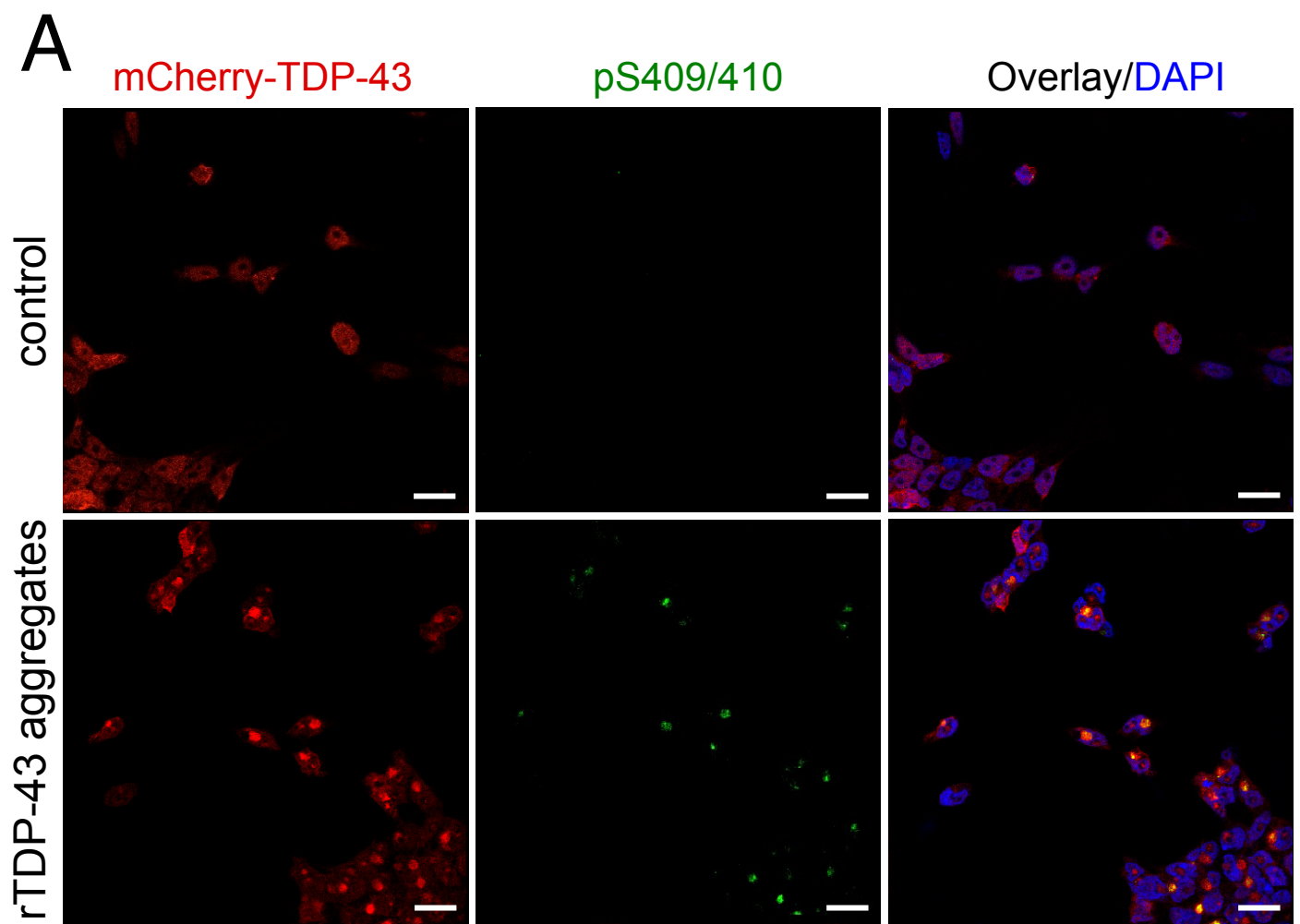
SUMO-less TDP-43



A**B**

Supp. Fig. 3





Supporting Figure Legends

Figure S1. Production of soluble recombinant TDP-43. (A) Recombinant TDP-43 expressed in bacteria purified on a nickel-charged affinity column. Representative SDS-PAGE and Coomassie blue staining of the purification samples. Arrow points to the eluted rTDP-43 fraction. (B) Removal of the SUMO tag following expression carried out on SUMO-TDP-43 immobilized on nickel-charged beads. Recombinant His-tagged Ulp1 protease was added to the beads and rTDP-43 (arrow) was recovered from the supernatant as shown in the representative Coomassie blue stained SDS-PAGE. (C) Fluorescence-based assay to measure TDP-43 RNA binding affinity for GU-repeats and estimate the active concentration of TDP-43. Representative plot of the intrinsic fluorescence (F) of recombinant TDP-43 upon titration of $(UG)_6$ RNA normalized by the fluorescence in the absence of RNA (F_0). Shown are F/F_0 values at four different TDP-43 concentrations and data were analyzed as previously described [21]. The best fit values for the apparent equilibrium dissociation constant, $K_{d,app}$ is 2.6 ± 0.5 .

Figure S2. TDP-43 oligomerization and aggregation does not depend on the presence of the N-terminal SUMO tag. Aggregation assays of TDP-43 analyzed by SDD-AGE/immunoblotting. (A) The crowding agent 0.7% PEG was added to the aggregation reaction to determine its effect on complex formation and rate of assembly. Markers to the left show the approximate molecular weight in kDa obtained from the migration of a pre-stained molecular weight marker. (B) Aggregation assays were carried out in the absence of the SUMO tag, as in Fig. 1A.

Figure S3. TDP-43 aggregates do not bind Thioflavin dyes. (A) Fluorescence Soluble recombinant TDP-43 (0.5 μ M) was incubated with increasing concentrations of Thioflavin-T (ThioT) for 2 hours in 18mM MES, pH 6.1, 5mM Tris, pH 8.0, 50mM NaCl, 1% Glycerol, 1% Sucrose, 30mM Imidazole at approximately 22°C. As control, ThioT binding experiments were carried out with 0.5 μ M recombinant α -synuclein under the same conditions. (B) Immunofluorescence microscopy of HEK-TDP-43^{NLS} treated with sodium arsenite (0.5 mM, 30 min). Arrowheads point to mCherry-positive, TDP-43 cytoplasmic inclusions also detected by the marker of TDP-43 pathology pSer409/410. Dashed lines delineate nuclear compartments.

Figure S4. Cellular reporter for TDP-43 aggregation HEK-TDP-43^{NLS}. (A) mCherry-tagged TDP-43 transgene stably expressed in HEK293 carrying amino acid substitutions to disrupt the nuclear localization sequence (NLS). Basic residues (Red) were changed to Ala. (B) Induced expression of mCherry-TDP-43^{NLS} visualized by fluorescence microscopy using DAPI to highlight nuclei. (C) Cells treated with 10 mM MG-132 for 16 hours and 0.5 mM sodium arsenite (NaAsn) for 30 minutes result in cytoplasmic aggregates which are recognized by the TDP-43 pathology marker pSer409/410. Overlay shows additional merging with DAPI. (D) Higher magnification of stress treated cells containing cytoplasmic aggregates. Scale bar, 10mm. (E) Lysate fractionation from control and MG-132/NaAsn treated cells into RIPA soluble and insoluble pellet resuspended in urea. Urea sample is 5-fold more concentrated than Total and RIPA samples. Samples loaded on SDS-PAGE and immunoblot probed with TDP-43 antibody.

S. Figure 5. TDP-43 seeding in HEK-TDP-43^{NLS} causes formation of pathologically relevant aggregates. Immunofluorescence of HEK-TDP-43^{NLS} cells transfected with rTDP-43-derived aggregates result in mCherry-positive aggregates. These inclusions are recognized by the TDP-43 pathology marker pSer409/410. Overlay shows additional merging with DAPI. (B) Higher magnification of stress treated cells containing cytoplasmic aggregates. Scale bar, 10 mm.